Triboelectric Nanogenerator Based on a Rotational Magnetic Ball for Harvesting Transmission Line Magnetic Energy

Xu Jin, Zhihao Yuan, Yapeng Shi, Yanggui Sun, Ruonan Li, Junhuan Chen, Longfei Wang, Zhiyi Wu,* and Zhong Lin Wang*

Triboelectric nanogenerators (TENGs) are attractive in powering sensors for smart power grids. Herein, a TENG based on a rotational magnetic ball is presented to harvest the magnetic energy of transmission lines. The magnetic ball rolls in a spherical shell under the alternating magnetic field generated by the transmission line. The centrifugal force produced during the rotation is used to drive a TENG unit (ten times the weight of the magnetic ball and shell) to generate electricity with the assistance of coil springs. The device can maintain the stability of the output performance under high current shocks; meanwhile, the open-circuit voltage, output power, and operating frequency of a single TENG unit can reach 1.5 kV, 6.67 mW, and 20 Hz, respectively. Furthermore, a wireless alarm system for monitoring the temperature and dip angle of transmission lines is successfully driven by this device. This work demonstrates an efficient and nontraditional strategy for harvesting magnetic energy through TENG, which is applied to power-distributed and self-powered sensors for monitoring transmission lines.

1. Introduction

With the rapid construction of the power grid, using sensors, communications technology, and other methods is required to realize the transmission network digital intelligence and the smart power grid.[1] In the power grid environment, there are a large number of extensive power resources, however, the power system for the sensors of transmission lines has some limitations.[2] The traditional power supply mode needs a lot of wirings and it would be practically impossible for this huge workload. The mode of power by using lifetime-limited batteries could not meet the long-term reliable work of the sensors.[3] In view of these problems, it is pressing to develop a sustainable power supply system to power sensors.

In recent years, it is a feasible and promising solution to harvest energy from a variety of environments. Compared with other environmental energies, such as wind energy and vibrational energy, the alternating magnetic energy generated by transmission lines could exist more widely and stably. At present, harvesting energy from alternating magnetic fields is mainly based on electromagnetic induction.[4] But electromagnetic coil must correspond to the range of current intensity of transmission lines or it can be a safety hazard, and the installation is complex.[5] Magnetic–mechanical–electric generators (MMEGs) based on the piezoelectricity effect can scavenge electricity from the magnetic fields generated by AC and have attracted great attentions.[6] Nevertheless, piezoelectric materials applied in MMEGs might need to sustain large mechanical strain and overcome mechanical fragility.[7]

Triboelectric nanogenerators (TENGs), based on triboelectrification and electrostatic induction, originate from the Maxwell's displacement current[8] and are widely applied in energy harvesters[9] and self-powered sensors.[10] TENG for harvesting magnetic energy on transmission lines has the merits of large design flexibility,[11] simple structure, lightweight, abundant choice of materials,[12] and low cost. The cantilever structure is a typical mode for harvesting magnetic energy for MMEGs that can easily respond to excitations from the magnetic fields,

X. Jin, Z. Yuan, Y. Shi, Y. Sun, R. Li, J. Chen, L. Wang, Z. Wu, Z. L. Wang
Beijing Institute of Nanoenergy and Nanosystems
Chinese Academy of Sciences
Beijing 100083, P. R. China
E-mail: wuzhiyi@binn.cas.cn
X. Jin, Z. Yuan, R. Li, Z. L. Wang
Center on Nanoenergy Research
School of Physical Science and Technology
Guangxi University
Nanning 530004, P. R. China
Y. Shi, Z. Wu, Z. L. Wang
College of Nanoscience and Technology
University of Chinese Academy of Sciences
Beijing 100049, P. R. China
Z. Wu, Z. L. Wang
CUSTech Institute
Wenzhou, Zhejiang 325024, P. R. China
Z. L. Wang
School of Materials Science and Engineering
Georgia Institute of Technology
Atlanta, GA 30332-0245, USA
E-mail: zlwang@gatech.edu

one end of the cantilever beam with permanent magnets is free and the other end is the fixed support. Chen et al. successfully designed a TENG based cantilever structure and suggested a new self-powered micro-weighing system.[13] Lim et al. introduced accelerated water-soluble nano-bullet to modify perfluoroalkoxy film nanostructures and demonstrated a TENG with cantilever structure.[14] However, the working principle of cantilever structure, based on vibrating at the resonant frequency of permanent magnets, leads to high requirements for the fixed segment and the material fatigue of the crucial working parts.

Considering the above-mentioned problems, a new structure could maintain the stability of the output performance under high current shocks and a prospective route and a non-traditional method should be proposed. In this work, a rotational magnetic ball[15] for TENG (RB-TENG) to harvest the alternating magnetic field is designed and fabricated. The magnetic ball could rotate around the center of itself under the magnetic field generated by the transmission current. With the friction between the magnetic ball and the spherical shell, then the magnetic ball would roll in a circle on the inside wall of the spherical shell. Benefitting from the rotation, the centrifugal force drives the two triboelectric layers to contact and separate with the assistance of coil springs to generate AC power. The RB-TENG can be activated at the magnetic field of transmission current and maintain the stability of the output performance under a high current shock (400 A). In this paper, the structure of RB-TENG is analyzed by COMSOL simulation and the output performance of the RB-TENG is systematically measured. The open-circuit voltage, short-circuit current, output power, and operating frequency of a single TENG unit can reach 1.5 kV, 20 μA, 6.67 mW, and 20 Hz. Next, the influence of the installation for RB-TENG in the magnetic field is investigated and shows the RB-TENG could efficiently harvest magnetic energy without high installation accuracy. Finally, a self-powered transmission line information detection/display/alarm system driven by the power-managed RB-TENG is fabricated as the demonstrated applications.

2. Results and Discussion

2.1. Composition and Working Illustration of the RB-TENG

The RB-TENG is setting on a transmission tower for harvesting magnetic energy of AC transmission lines (**Figure 1**a). The basic structure of the RB-TENG is mainly composed of a motor unit, a TENG unit, and a baffle unit (Figure 1b and Figure S1). The centrifugal force generated by the magnet ball rotation can easily drive the triboelectric layers to carry out the contact and separation states (ten times the weight of the magnetic ball and shell, Figure S2). To make good use of the centrifugal force, three coil springs are installed on the bottom of the acrylic spherical shell. It is worth mentioning that the wire diameter of the three coil springs cannot be lower than 0.4 mm, or the magnetic ball would not roll spontaneously under the action of the alternating magnetic field. Because the three coil springs not only determine the stability of the acrylic spherical shell but also have influences on the friction force between the magnetic ball and the spherical shell that plays an important role in the rotation process. For the TENG unit, to increase the contact area and improve output power, two coil springs are used to support the triboelectric layer that is adhered to the spherical shell and four coil springs are used to connect the other triboelectric layer to the baffle unit. With the supporting springs, the output value of voltage and current can reach 1.5 kV and 20 μA, which are much larger than 200 V and 6 μA (without the support springs, Figure S3). A working framework for harvesting magnetic field energy of transmission line based on RB-TENG is illustrated (Figure 1c).
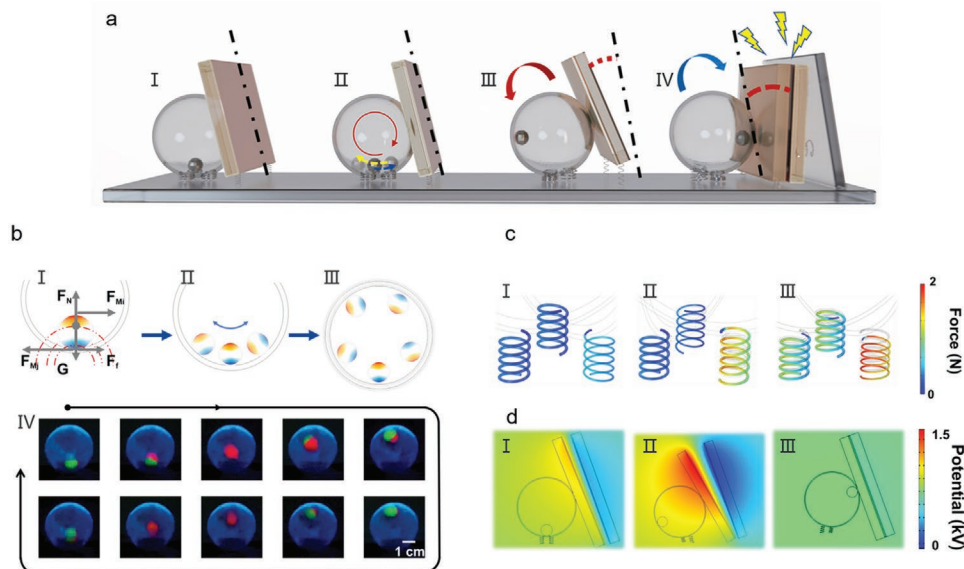
2.2. Working Mechanism of the RB-TENG

There are four typical locations during the whole process of harvesting magnetic energy (I: the initial state; II: startup stage; III and IV: steady rotation stage. **Figure 2**a). The mechanics analysis diagram of the magnetic ball at a special position in the initial state is illustrated (Figure 2bI). Under this condition, the gravity (G) is equal to the supporting force (F_N). The magnetic
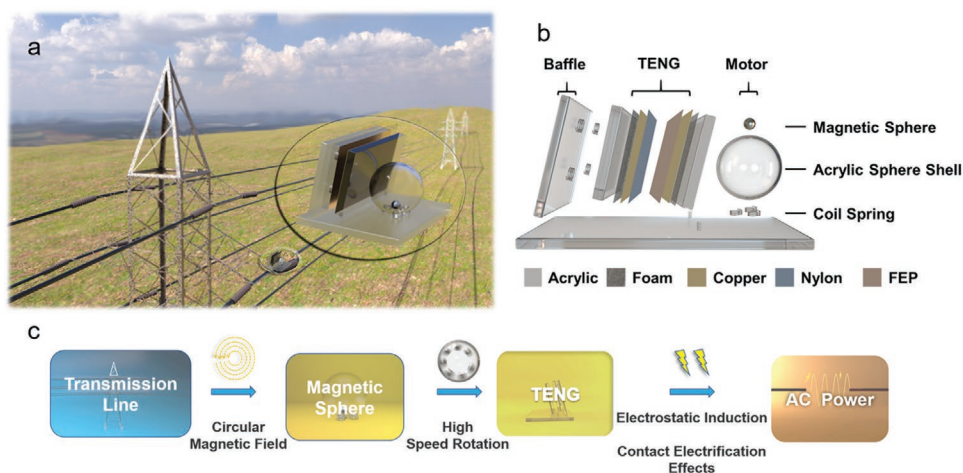
Figure 1. Structure and illustration of the RB-TENG. a) Schematic diagram of the RB-TENG setting on a transmission tower, and the enlarged structure of RB-TENG. b) Schematic structure of RB-TENG. c) Framework for collecting magnetic field energy of transmission line based on RB-TENG.

Figure 2. Illustration of the working mechanism of the RB-TENG. a) Schematic exhibiting various motion patterns of the RB-TENG under alternating magnetic field generated by the transmission line. b) I Mechanics analysis diagram of the magnetic ball. II Schematic diagram of the motion state of the magnetic ball in the startup stage of the movement of RB-TENG. III stabilization stage. IV Photographs of the magnetic ball in the stable rotation stage. c) The mechanical simulation results of the coil springs supporting the spherical shell in operation using COMSOL. d) Electrostatic potential distributions at three typical positions.

pole closed to the transmission line receives a magnetic force of F_{Mj} and the other pole receives a smaller magnetic force of F_{Mi}. Therefore, the magnetic ball would rotate around the center of itself. In the startup stage, the magnetic ball rolls randomly at the bottom of the shell. With the rolling speed of the magnetic ball increasing, the pressure of the magnetic ball on the acrylic sphere shell could increase continuously, then the magnetic ball would roll in a circle on the inside wall of the spherical shell with the assistance of the friction. To observe and verify the whole process, fluorescent paint is used to mark the poles of the magnetic ball and the process from startup stage to steady rotation stage is recorded in slow motion (Movie S1, Supporting Information). A series of photographs of a magnetic ball rotating during one period are shown in Figure 2b IV. Considering the stability and mobility of the spherical shell, a triangular distribution structure for the springs is used. The side with one single spring is more likely to deform and make the shell move than the side with double springs. For demonstrating the performance of these springs, the relationship between force and deformation of the springs with the mover moving to different places under the ideal centrifugal force is simulated by COMSOL Multiphysics 5.5 (Figure 2c). Moreover, Figure 2d describes the simulation results by using the COMSOL Multiphysics 5.5 of three typical electrostatic voltage distributions with the RB-TENG on the initial state and steady rotation stage. Under the triggering of rotation, the contact and separation between the nylon film and fluorinated ethylene propylene film generate opposite charges on their surfaces and the change of the electrical potential (Figure S4).
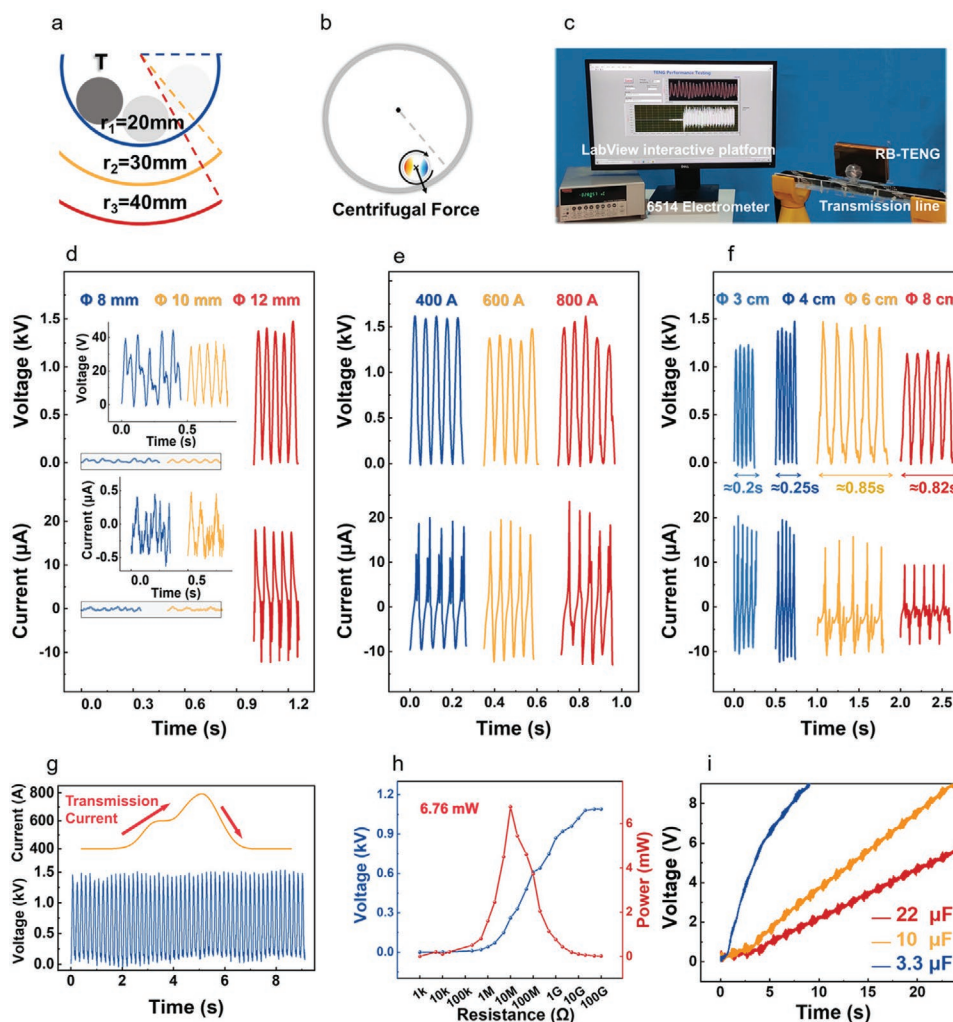
2.3. The Output Performance Measurement of the RB-TENG

The magnetic balls, the spherical shells (Figure S5), and the transmission lines (Figure S6) would be the crucial parameters

governing the output performance of the TENG unit (**Figure 3**a,b). To verify the effect of magnetic balls on the output performance of RB-TENG, a spherical shell with a diameter of 4 cm is utilized, and the magnetic field is generated by a 600 A transmission line (Figure 3c). As the diameter of the magnetic ball increases from 8 to 12 mm, the open-circuit voltage and short-circuit current enhance obviously (Figure 3d), which could reach 1.5 kV and 20 µA (Movie S2, Supporting Information) at the magnetic ball with a diameter of 12 mm and are much higher than the others (40 V and 0.5 µA). That is because the magnetism and the mass of a magnetic ball are positively related to the cubic of its radius, which are positive relations to the output performance of the RB-TENG.

In addition, to investigate the effect of magnetic fields on the output performance of RB-TENG, a magnetic ball with a diameter of 12 mm and a spherical shell with a diameter of 4 cm are utilized to fabricate RB-TENG. Interestingly, as the current in the transmission line increasing from 400 to 800 A, the output performance of the TENG unit does not change significantly (≈1.5 kV and 20 µA, Figure 3e). The results prove that the RB-TENG could accommodate a wide range of transmission currents.

The effect of shell on the output performance of RB-TENG is also explored (Figure 3f and Figure S7). The diameter of the magnetic ball is set as 12 mm, and the magnetic field is generated by 600 A transmission line. It is evident that the operating frequency of RB-TENG sharply reduces from ≈20 to 5.8 Hz with no remarkable changes in electrical output when the diameter of the shell increases from 4 to 6 cm. The operating frequency of RB-TENG could not increase obviously with 3 cm. The RB-TENG has the better excellent working performance with 4 cm shell. When the diameter of spherical is selected as 8 cm, the open-circuit voltage of RB-TENG has slightly reduced to 1.2 kV, which is attributed to the decay of the centrifugal force to the magnetic ball when it is farthest from the transmission line.

**ADVANCED
SCIENCE NEWS**

www.advancedsciencenews.com

**ADVANCED
FUNCTIONAL
MATERIALS**

www.afm-journal.de

Figure 3. The output performance of the RB-TENG. a,b) Mechanical analysis. c) Photograph of the test platform. d) Short-circuit current and open-circuit voltage of the RB-TENG at various magnetic ball diameters. e) Short-circuit current and open-circuit voltage of the RB-TENG at various transmission currents. f) Short-circuit current and open-circuit voltage of the RB-TENG at various spherical shell diameters. g) The voltage curve of RB-TENG under a high current shock. h) Output power-resistance profiles. i) Charging voltage on various load capacitors.

Considering the current of the transmission line is dynamic and a huge current shock (400 A) is also set to verify the stability of the RB-TNG. Surprisingly, the output performance of RB-TENG has no obvious fluctuation under such a schematic high current shock (Figure 3g). The current shock would accelerate the rotation of the magnetic ball and make the centrifugal force increase. However, the output performance of RB-TENG had already reached the maximum value. This suggests that the RB-TENG has excellent stability under this destructive current shock. For this constructed RB-TENG, maximum output performance could be obtained and the structure can adapt to the magnetic fields generated by the whole range of transmission lines over 400 A by using a magnetic ball with a diameter of 12 mm and a spherical shell with a diameter of 4 cm. The output peak power–resistance relationship and the charging curves for various electrolytic capacitors are shown in Figure 3h,i. Additionally, the voltage of the output peak power–resistance relationship is measured by an oscilloscope (Figure S8) and the maximum output peak power arrives at 6.67 mW at the

matched resistance of 10 MΩ. And the voltage of the capacitor of 22 µF can be raised to 3 V within 15 s. These results demonstrate the feasibility of powering various sensors.

2.4. The Effects of the Installation and Output Performance of the RB-TENG

Due to the characteristic of the magnetic field generated by the transmission line, the installation position of the device is a considerable factor for harvesting the magnetic energy of the transmission line. For the RB-TENG, if the shell is fixed without springs, the magnetic ball would roll steadily at a certain path on the inner wall of the shell (**Figure 4**a). However, when the shell is fixed with springs, the rotation of the magnetic ball would cause the shell to move in the alternating magnetic field, and the offset of the shell would have huge influences on the position and the force of the magnetic ball, then the rolling path of the magnetic ball would be complex and unpredictable.
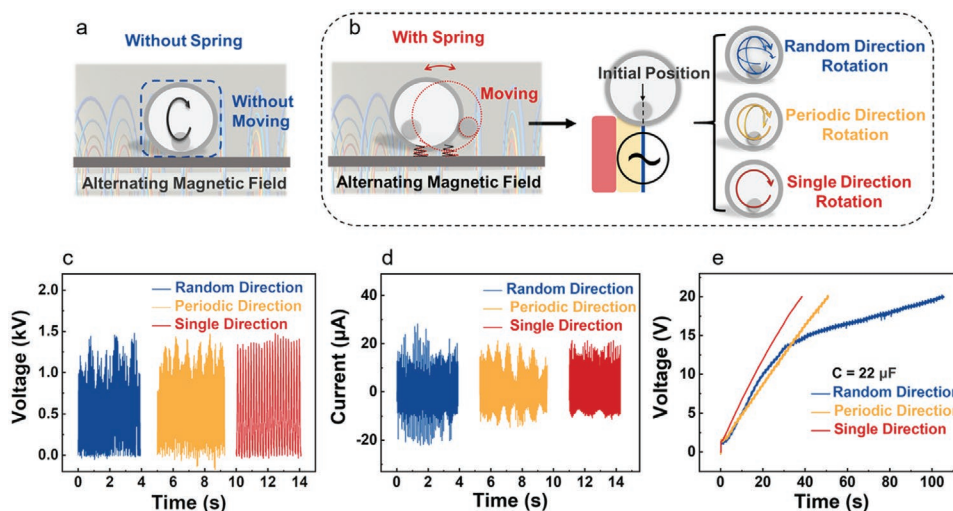
Figure 4. The effects of the installation and output performance of the RB-TENG. a,b) Analysis of the various directions of rotation of the magnetic ball. c) The open-circuit voltage, d) the short-circuit current, and e) charging voltage on 22 μF load capacitor for various directions of rotation.

Although this effect is hard to erase, the rotation path can be adjusted into three modes to some extent by changing the initial position (Movie S3, Supporting Information). As the initial position is away from the center of the transmission line, the influence of offset of the shell on the magnetic ball decreases continuously (Figure 4b). The circular rotation path of the magnetic ball would randomly change when the initial position of the magnetic ball is centered with the transmission line. The circular rotation path of the magnetic ball changes periodically when the initial position of the magnetic ball is above the transmission line but not at the center. The magnetic ball will roll in one single direction when the initial position is not above the transmission line.

To obtain a more quantitative understanding about the influence of the installation position of the device, the electrical output performance and the charging curves for an electrolytic capacitor of 22 μF are described in Figure 4c,d. When the magnetic ball rolls in random directions or periodic directions, the maximum voltage and current could reach 1.5 kV and 27 μA but which are with a huge difference between the maxima and the minima of the voltage and current. The stable and high electrical output can be obtained when the magnetic ball rolls in one single direction. As shown in Figure 4e, for the storage capacitor of 22 μF, various rotation modes have little effect for harvesting magnetic field energy in 40 s, although the impact cannot be ignored for long-term harvesters. As can be seen, the range of installation positions for the device is wide and uncomplicated, and the device could efficiently harvest magnetic energy without high installation accuracy.

2.5. Applications of the RB-TENG

Basing on RB-TENG, a variety of applications including detection, display, temperature, and dip angle monitoring for transmission line is realized (**Figure 5**a). A temperature trigger and a dip angel trigger are used as the control units to build a self-powered temperature alarm/dip angle system for transmission

line (Figure S9), in which the schematic diagram is presented in Figure 5b. When the temperature/dip angle is higher than the trigger threshold, a wireless transmitter controlled by a microcontroller unit will send a control command, which would be received by a wireless receiver to help a bell ring and light-emitting diodes (LEDs) light (Movie S4, Supporting Information). The photographs and typical working waveforms of the temperature alarm/dip angle alarm system are plotted in Figure 5c. The voltage on the energy storage unit can rapidly reach 3.3 V within the charging time of 35 s, which is the operating voltages of the microcontroller unit and the wireless transmitter are 3.3 V.

As an intuitive demonstration of the excellent performance, the application of powering 35 LEDs is also shown in Figure 5d and Movie S5, Supporting Information. A self-powered digital thermometer is constructed and the typical working waveforms and the corresponding photographs are demonstrated in Figure 5e. A storage capacitor of 470 μF is charged to 1.3 V within 88 s (Figure 5eI), then the thermometer could be powered constantly by RB-TENG (Figure 5e and Movie S6, Supporting Information) and the voltage value is stable at 1 V. Considering the high output and scalable property of RB-TENG, different scales of device networks can be developed and applied for transmission line self-powered systems, which are of great value in transmission line researches, smart power grids, and clean energy exploitations.

3. Conclusions

In summary, TENG with a new structure to harvest magnetic energy of transmission line is designed and fabricated, based on a magnetic ball, which is the core component of the RB-TENG to respond to the magnetic field and generate centrifugal force. The RB-TENG could be activated at the magnetic field of transmission current over 400 A and maintain the stability of the output performance under a high current shock (400 A). The maximum outputs of 1.5 kV, 20 μA, 6.67 mW, and 20 Hz
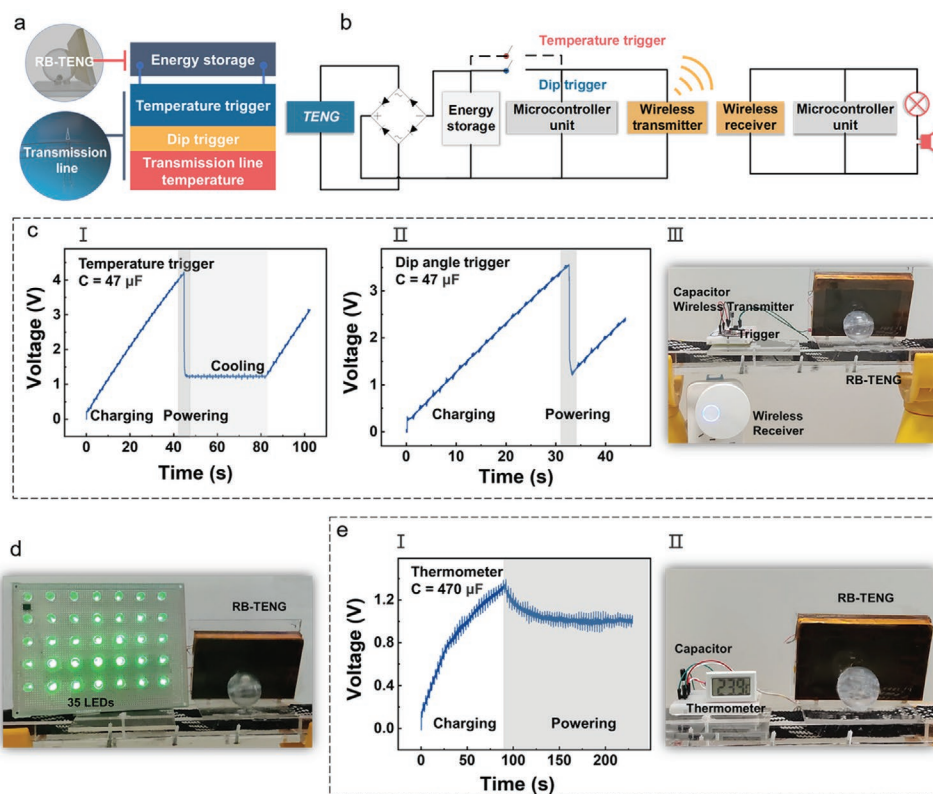
Figure 5. The applications of the RB-TENG. a) Framework for the integrated self-powered transmission line information detection/display/alarm system driven by the power-managed TENG. b) Schematic diagram of a self-powered wireless alarm system for monitoring temperature and dip angle of the transmission line. c) Typical working waveform and photographs of the temperature and dip angle alarm system. d) Powering 35 LEDs by a single device. e) Typical working waveform and photographs of the thermometer.

are obtained at the magnetic ball with a diameter of 12 mm and the spherical shell with a diameter of 4 cm. Meanwhile, a wide range of transmission currents could be accommodated and the operating frequency of the TENG unit is directly controlled by the diameter of the spherical shell. Then the influence of the initial installation position of the device is studied, which shows the device could efficiently harvest magnetic energy without high installation accuracy. Finally, a self-powered transmission line information detection/display/alarm system driven by the power-managed RB-TENG has been built and tested, which confirmed the technical feasibility of the device for powering distributed, self-powered sensors of transmission line monitoring.

4. Experimental Section

Fabrication of the PR-TENG: The motor unit was 13 g, including a permanent magnet ball (NdFeB, N35), an acrylic spherical shell (2 mm thick), and three coil springs. The acrylic spherical shell was fixed to the acrylic sheet (3 mm) by three 304 stainless steel coil springs (Figure S1) distributed 120° apart along a 12 mm diameter circle. The triboelectric layer was 130 g and laminated by an acrylic substrate (13 cm × 8.5 cm × 1 cm), a sponge layer (1 mm), a copper film (30 μm), a FEP film (80 μm), or a nylon film (30 μm). The baffle unit was made of acrylic sheets with the thick of 3 mm. The layers of nylon and FEP were commercial thin films without corona charged.

Characterization and Measurement: The electrical output performance of RB-TENG was measured by using an electrometer (KEITHLEY Model 6514 system electrometer), a data acquisition card (NI PCIe-6376), and an oscilloscope (KEYSIGHT DSOX2024A). In the experiment, the current of the transmission current was simulated by an AHY-12 series linear AC adjustable constant current source. The alarm system was obtained from LINPTECH (G6L-SW).

Supporting Information

Supporting Information is available from the Wiley Online Library or from the author.

Conflict of Interest

The authors declare no conflict of interest.

Data Availability Statement

Research data are not shared.

Keywords

[1] a) M. M. Werneck, D. Moreira dos Santos, C. Cosenza de Carvalho, F. Vieira Batista de Nazare, R. Celia da Silva Barros Allil, *IEEE Sens. J.* **2015**, *15*, 1338; b) Z. Wu, T. Cheng, Z. L. Wang, *Sensors* **2020**, *20*, 2925.

[2] J. Zhou, Y. S. Geng, X. G. Wang, *Appl. Mech. Mater.* **2013**, *321–324*, 1396.

[3] Z. L. Wang, J. Chen, L. Lin, *Energy Environ. Sci.* **2015**, *8*, 2250.

[4] Z. Wu, Y. Wen, P. Li, *IEEE Trans. Energy Convers.* **2013**, *28*, 921.

[5] D. Mallick, P. Constantinou, P. Podder, S. Roy, *Sens. Actuators, A* **2017**, *264*, 247.

[6] a) J. Ryu, J.-E. Kang, Y. Zhou, S.-Y. Choi, W.-H. Yoon, D.-S. Park, J.-J. Choi, B.-D. Hahn, C.-W. Ahn, J.-W. Kim, Y.-D. Kim, S. Priya, S. Y. Lee, S. Jeong, D.-Y. Jeong, *Energy Environ. Sci.* **2015**, *8*, 2402; b) Y. Hu, Z. L. Wang, *Nano Energy* **2015**, *14*, 3.

[7] a) Y. Nan, D. Tan, J. Shao, M. Willatzen, Z. L. Wang, *ACS Energy Lett.* **2021**, *6*, 2313; b) G.-T. Hwang, V. Annapureddy, J. H. Han, D. J. Joe, C. Baek, D. Y. Park, D. H. Kim, J. H. Park, C. K. Jeong, K.-I. Park, J.-J. Choi, D. K. Kim, J. Ryu, K. J. Lee, *Adv. Energy Mater.* **2016**, *6*, 1600237.

[8] Z. L. Wang, *Mater. Today* **2017**, *20*, 74.

[9] a) Z. Wu, W. Ding, Y. Dai, K. Dong, C. Wu, L. Zhang, Z. Lin, J. Cheng, Z. L. Wang, *ACS Nano* **2018**, *12*, 5726; b) Z. Wu, H. Guo, W. Ding, Y. C. Wang, L. Zhang, Z. L. Wang, *ACS Nano* **2019**, *13*, 2349; c) X. Liang, T. Jiang, G. Liu, Y. Feng, C. Zhang, Z. L. Wang, *Energy Environ. Sci.* **2020**, *13*, 277; d) H. Wang, L. Xu, Y. Bai, Z. L. Wang, *Nat. Commun.* **2020**, *11*, 4203; e) W. Yang, J. Chen, G. Zhu, X. Wen, P. Bai, Y. Su, Y. Lin, Z. Wang, *Nano Res.* **2013**, *6*, 880; f) P. Cheng, H. Guo, Z. Wen, C. Zhang, X. Yin, X. Li, D. Liu, W. Song, X. Sun, J. Wang, Z. L. Wang, *Nano Energy* **2019**, *57*, 432; g) J. Chung, H. Yong, H. Moon, Q. V. Duong, S. T. Choi, D. Kim, S. Lee, *Adv. Sci.* **2018**, *5*, 1801054; h) W. Liu, Z. Wang, G. Wang, G. Liu, J. Chen, X. Pu, Y. Xi, X. Wang, H. Guo, C. Hu, Z. L. Wang, *Nat. Commun.* **2019**, *10*, 1426; i) H. Guo, J. Chen, L. Wang, A. C. Wang, Y. Li, C. An, J.-H. He, C. Hu, V. K. S. Hsiao, Z. L. Wang, *Nat. Sustainability* **2020**, *4*, 147; j) X. He, H. Guo, X. Yue, J. Gao, Y. Xi, C. Hu, *Nanoscale* **2015**, *7*, 1896; k) J. Chen, H. Guo, X. He, G. Liu, Y. Xi, H. Shi, C. Hu, *ACS Appl. Mater. Interfaces* **2016**, *8*, 736; l) G. Zhu, Z. H. Lin, Q. Jing, P. Bai, C. Pan, Y. Yang, Y. Zhou, Z. L. Wang, *Nano Lett.* **2013**, *13*, 847.

[10] a) B. Zhang, Z. Wu, Z. Lin, H. Guo, F. Chun, W. Yang, Z. L. Wang, *Mater. Today* **2021**, *43*, 37; b) R. Li, X. Wei, J. Xu, J. Chen, B. Li, Z. Wu, Z. L. Wang, *Micromachines* **2021**, *12*, 1308. c) H. Guo, X. Pu, J. Chen, Y. Meng, M.-H. Yeh, G. Liu, Q. Tang, B. Chen, D. Liu, S. Qi, C. Wu, C. Hu, J. Wang, Z. L. Wang, *Sci. Rob.* **2018**, *3*, eaat2516; d) H. Guo, M. H. Yeh, Y. Zi, Z. Wen, J. Chen, G. Liu, C. Hu, Z. L. Wang, *ACS Nano* **2017**, *11*, 4475; e) Q. Gao, T. Cheng, Z. L. Wang, *Extreme Mech. Lett.* **2021**, *42*, 101100.

[11] a) F.-R. Fan, Z.-Q. Tian, Z. L. Wang, *Nano Energy.* **2012**, *1*, 328; b) Z. L. Wang, L. Lin, J. Chen, S. Niu, Y. Zi, *Triboelectric Nanogenerators*, Springer, New York **2016**.

[12] H. Zou, Y. Zhang, L. Guo, P. Wang, X. He, G. Dai, H. Zheng, C. Chen, A. C. Wang, C. Xu, Z. L. Wang, *Nat. Commun.* **2019**, *10*, 1427.

[13] J. Chen, H. Guo, Z. Wu, G. Xu, Y. Zi, C. Hu, Z. L. Wang, *Nano Energy* **2019**, *64*, 103920.

[14] K.-W. Lim, M. Peddigari, C. H. Park, H. Y. Lee, Y. Min, J.-W. Kim, C.-W. Ahn, J.-J. Choi, B.-D. Hahn, J.-H. Choi, D.-S. Park, J.-K. Hong, J.-T. Yeom, W.-H. Yoon, J. Ryu, S. N. Yi, G.-T. Hwang, *Energy Environ. Sci.* **2019**, *12*, 666.

[15] a) H. Wu, A. Tatarenko, M. I. Bichurin, Y. Wang, *Nano Energy* **2021**, *83*, 105777; b) S. Hajra, V. Vivekananthan, M. Sahu, G. Khandelwal, N. P. M. Joseph Raj, S.-J. Kim, *Nano Energy* **2021**, *85*, 105964.